International Journal of Refrigeration 133 (2022) 61–72

Contents lists available at ScienceDirect

International Journal of Refrigeration

journal homepage: www.elsevier.com/locate/ijrefrig

Energy, exergy, and environmental (3E) analysis of a compound ejector-heat pump with low GWP refrigerants for simultaneous data center cooling and district heating

Analyse énergétique, exergétique et environnementale (3E) d'une pompe à chaleur composée à éjecteur fonctionnant avec des frigorigènes à faible PRP pour le refroidissement d'un centre de données et le chauffage urbain simultanés

Ali Khalid Shaker Al-Sayyab [a,b], Joaquín Navarro-Esbrí [a], Adrián Mota-Babiloni [a,*]

[a] ISTENER Research Group, Department of Mechanical Engineering and Construction, Universitat Jaume I, Campus de Riu Sec s/n, 12071 Castellón de la Plana, Spain
[b] Basra Engineering Technical College (BETC), Southern Technical University, Basra, Iraq

ARTICLE INFO

Keywords:
Low GWP refrigerants
Data center cooling
Photovoltaic thermal (PV/T)
3E assessment
Compound ejector-vapor compression
R134a alternatives

Mots clés:
Frigorigènes à faible PRP
Refroidissement des centres de données
Photovoltaïque thermique (PV/T)
Évaluation 3E
Systèmes composés à éjecteur et à compression de vapeur
Alternatives au R134a

ABSTRACT

This work presents an energy, exergy, and environmental evaluation of a novel compound PV/T (photovoltaic thermal) waste heat driven ejector-heat pump system for simultaneous data center cooling and waste heat recovery for district heating networks. The system uses PV/T waste heat with an evaporative-condenser as a driving force for an ejector while exploiting the generated electric power to operate the heat pump compressor and pumps. The vapor compression system assessed several environmentally friendly strategies. The study compares eleven lower global warming potential (GWP) refrigerants from different ASHRAE safety groups (R450A, R513A, R515A, R515B, R516A, R152a, R444A, R1234ze(E), R1234yf, R290, and R1243zf) with the hydrofluorocarbon (HFC) R134a. The results prove that the system presents a remarkable overall performance enhancement for all investigated refrigerants in both modes. Regarding the energy analysis, the cooling coefficient of performance (COP_C) enhancement ranges from 15% to 54% compared with a traditional R134a heat pump. The most pronounced COP_C enhancement is caused by R515B (a 54% COP_C enhancement and 49% heating COP enhancement), followed by R515A and R1234ze(E). Concerning the exergy analysis, R515B shows the lowest exergy destruction, with the highest exergy efficiency than all investigated refrigerants.

1. Introduction

The world needs to cut greenhouse gas emissions in half by 2030 and work towards carbon neutrality by 2050 to avoid major disasters (GlobalABC/IEA/UNEP, 2020). An immediate increase in demand for energy-consuming services due to an increasing population density and life evolution are outpacing efficiency improvements and heat decarbonisation. The International Energy Agency (IEA) has proposed a pathway for a sustainable development scenario, focuses on reducing electricity dependence by increasing renewable energy sources usage, enhancing energy efficiency, and recovering waste heat (*IEA, World Energy Outlook 2019, IEA, Paris*, 2019); (OECD /IEA 2018). In this way, electricity decarbonisation represents around 30% of the emissions reductions needed (GlobalABC/IEA/UNEP, 2020).

By 2050, the European Union (EU) target is to become climate neutral by increasing renewable energy and improving energy efficiency. Focusing on refrigeration, heating, ventilation, and air-conditioning (RHVAC) systems, the Kigali Amendment to the Montreal protocol started the global hydrofluorocarbon (HFC) consumption phase-down in 2019. In this regard, R134a is one of the most common HFC refrigerants, with a global warming potential of 1430, which can be easily found in domestic refrigerators, medium temperature commercial applications, mobile air conditioning, water chillers and water-to-water heat pumps (Mota-Babiloni et al., 2017). Therefore, there is an urgent necessity of providing suitable, environmentally friendly alternatives. Besides,

* Corresponding authors.
E-mail address: mota@uji.es (A. Mota-Babiloni).

https://doi.org/10.1016/j.ijrefrig.2021.09.036
Received 28 April 2021; Received in revised form 29 September 2021; Accepted 30 September 2021
Available online 5 October 2021

Nomenclature

COP	Coefficient of performance (-)
EC	Energy consumption (kWh year^{-1})
h	Specific enthalpy (kJ kg^{-1})
I	Solar intensity (W m^{-2})
LK	Refrigerant system annual leakage rate (kg)
NBP	Normal boiling point (°C)
P	Pressure (MPa)
rpm	Revolution per minute
RT	Running time of the system (hour)
T	Temperature (°C)
V	Volume (m^3)
$\dot{E}X$	Exergy rate (kJ s^{-1})
$\dot{m}$	Refrigerant mass flow rate (kg s^{-1})
$\dot{Q}$	Heat transfer rate (kW)
$\dot{W}$	Electrical consumption power (kW)

Greek symbols

α	System operational lifetime (year)
β	Carbon emission factor (CO_2-eq kWh^{-1})
ε	Heat exchanger effectiveness (-)
η	Efficiency (-)
γ	Carbon emission factor (g kWh^{-1})
μ	Entrainment ratio (-)
ω	Refrigerant velocity (m s^{-1})

Subscripts

C	Compressor, Cooling mode
Cri	Critical condition
D	Diffuser, discharge
Des	Destruction
Ds	Displacement
e	Evaporator
ea	Actual exit condition
ej	Ejector
ek	Evaporative condenser
el	Electricity
em	Electromechanical
es	Isentropic exit condition
exp	Expansion valve
g	Generator
h	Hot stream, heating mode
HX	Heat exchanger
in	Inlet
is	Isentropic conditions
k	Condenser
l	Cold stream
m	Mixing conditions
n	Normal shock conditions
out	Outlet
p	Primary stream
pn	Primary nozzle
r	Refrigerant
s	Secondary stream, suction
sn	Suction nozzle
t	Total
v	Volumetric
w	Water stream
0	Dead state conditions

Abbreviatures

3E	Energy-exergy, and environmental
ASHRAE	The American Society of Heating, Refrigerating and Air-Conditioning Engineers
EES	Engineering equation solver
GHG	Greenhouse gases
GWP	Global warming potential
HFC	Hydrofluorocarbon
IEA	International energy agency
ODP	Ozone depletion potential
PV/T	Photovoltaic thermal
RHVAC	Refrigeration, heating, ventilation, and air conditioning
tCO_2-eq	Ton of equivalent carbon dioxide emissions
TEWI	Total equivalent warming impact

according to the IEA, RHVAC systems have to produce heating and cooling simultaneously to improve energy efficiency and efficiently use the resources (IEA, 2018) because these systems can save electricity compared to traditional heat pumps (Byrne and Ghoubali, 2019). A definitive transition to working fluids with a GWP below 150 would mitigate the climate impact significantly caused by these widespread systems (EEA, 2020).

Another way of improving RHVAC systems efficiency is by connecting it (hybridising) to renewable energy sources. Solar energy is the cleanest and most abundant renewable energy source and can be converted into thermal or electrical energy. Spain and other Southern countries have most of the richest solar resources in Europe (SOLARGIS, 2019). On the other hand, combining photovoltaic thermal (PV/T) technologies with heat pumps (named solar assisted heat pumps) can improve PV/T efficiency because their operating temperature is reduced. On the other hand, heat pump efficiency also increases because it operates at higher evaporating temperatures, absorbing less electric power than conventional heat pumps.

A few studies have evaluated the potential of solar assisted heat pumps in terms of energy efficiency increase. Bai et al. (2012) simulated and tested a solar-assisted R410A heat pump for hot water production that reduced electricity consumption and increased heating coefficient of performance (COP) by 67% and 49% compared to a conventional heating system. Fu et al. (2012) presented an energy and exergy assessment of a solar-assisted R134a heat pump system operated in three modes: heat-pipe and solar-assisted and air-source heat pumps. The solar-assisted heat pump mode exposed the highest average daily energy and exergy efficiencies, 37.5% and 7.6%, respectively.

The inclusion of an ejector in solar-assisted heat pump configurations could benefit the system performance. Hazi et al. (2014) compared PV/T assisted ejector heat pump systems with conventional heat pumps for paper mill application. They concluded that increasing hot water temperature would decrease both configurations energy, exergy, and economic performance. Moreover, the solar-assisted ejector heat pump was the most suitable technology. Boumaraf et al. (2016) modelled an ejector refrigerating system using a flat-plate solar collector with alternative refrigerants to R134a. The study observed that the R290 system showed the best performance of all investigated refrigerants. Xu et al. (2019) simulated an R600a system for cooling purposes. They proved that combining solar energy ends with higher energy and electrical performance than without it (11.8% electricity consumption reduction and 12.5% overall COP enhancement). Shaker Al-Sayyab et al. (2021) simulated a compound ejector-heat pump system with R450A and R513A that uses PV/T waste heat with a flat plate collector, milk pasteurisation process or a condenser. The study concluded that the R450A system resulted in a 75% system COP enhancement for the milk pasteurisation. In contrast, other studies explored the performance of compound vapour compression ejector systems when the generator

pumps are replaced by other technologies like a flash tank (Chen and Yu, 2017a), cascades, and a multi evaporator (Huang et al., 2018). All of them conclude that the combination has a positive effect on system energy performance.

Information and communications technology represent an emerging sector, representing 2.5% of total European Union electricity consumption (78 TWh) (European Commission, 2015). The Internet of Things (IoT) offers business opportunities and is guaranteed to improve efficiency, transparency, and security at any company. However, implementing IoT often involves exchanging big data and producing urgent data centres, increasing power demand between 15 and 20% (Avgerinou et al., 2017). One of the most critical data centres challenges is reducing the operating cost (electricity consumption) and the associated carbon footprint. The energy consumed by the data center is converted into excess heat, which is generally released to the cooling system ambient to prevent components damage and guarantee electronics performance (Davies et al., 2016). According to the Environmental Protection Agency (EPA), the relevance of these systems is that data centres constitute approximately 2% of the global CO_2-eq emissions, which are expected to grow in the coming years (GeSI. SMART 2020., 2008). The performance and lifetime of data center electronic components are susceptible to indoor conditions; therefore, cooling systems performance becomes one of the most critical challenges in data center design and operation (Mukaffi et al., 2017). The cooling system causes such an electricity consumption representing 40% of the total consumption, to counteract the data centre thermal load (Payerle et al., 2015).

Some studies highlighted the relevance of improving the cooling system energy efficiency by employing excess heat (waste heat recovery method). He et al. (2018) concluded that a data centre waste heat using heat pipe-heat pump arrangements for supporting district heating systems in different Chinese cities would reduce down to 10% energy consumption compared to heating based on traditional coal-powered boilers. Sheme et al. (2018) included two renewable energy sources for data centre cooling. The study predicted that the combined renewable sources provide more significant surplus hours than when considered independently.

The state-of-art revision shown in this section is imperative to reduce data centre cooling energy consumption. In this way, several methods have been proposed, including waste heat, new technologies or renewable energy sources. However, today data centre cooling systems do not include them, and environmental reports warn about the significant energy used and wasted for this application. Therefore, future proof systems with operation reliability, environmentally friendly must be proposed.

In this work, a new arrangement for a combined ejector-solar assisted heat pump system is proposed to be applied for simultaneous data center cooling and district heating. This novel arrangement combines five environmentally friendly promising technologies: heat pumps, ejectors, PV/T panels, waste heat recovery, and low GWP refrigerants. The proposed system presents the novelty of employing PV/T waste heat with the evaporative condenser as a full ejector driving force, avoiding a pump need. The surplus PV/T generated electricity can operate the heat pump, cooling a data center, and injecting heat in a district heating network. Data centre waste heat recovery could significantly reduce energy consumption and carbon footprint.

A new method involving advanced exergoeconomic analysis was recently adopted into the current system (Al-Sayyab et al., 2021). It evaluates exergoeconomic costs for each component at constant operating conditions (solar intensity, generator temperature, superheating degree) using solely R134a as the working fluid. Moreover, to comprehensively evaluate current system performance, the effect of several low global warming (GWP) refrigerants on the proposed system is investigated and compared with R134a. The influence of solar radiation is taking actual weather data of Valencia (Spain) to investigate the hourly performance in different seasons. The exergy analysis is combined with energy modelling and simulation techniques to identify the magnitude and sources of thermodynamics irreversibility in the proposed system and system performance evaluation. This work presents a 3E evaluation (energy, exergy and environmental) to give a complete overview of the proposed system configuration potential considering different external conditions and applications. Therefore, the main objectives of this work are as follows: to develop a new compound cooling system with lower power consumption and based on low GWP refrigerants; to use renewable energy as the electricity source for the cooling system; to improve data centre cooling efficiency; to recover and reuse waste heat from data

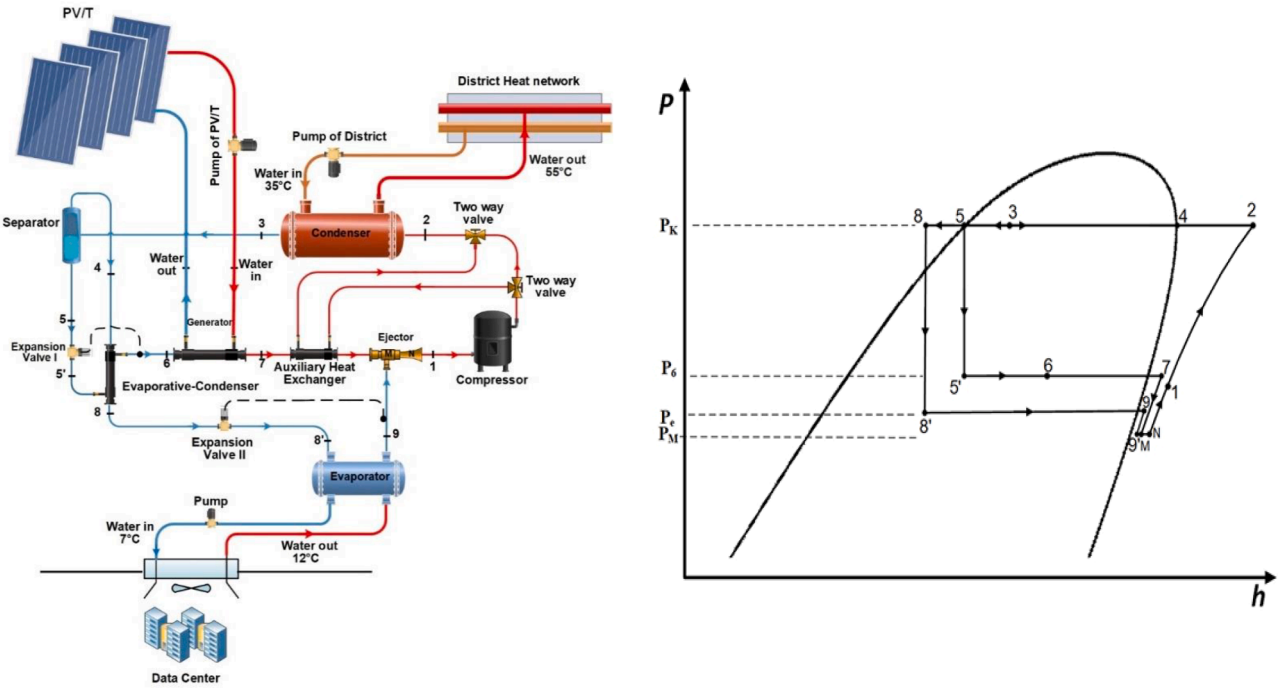

Fig. 1. Schematic and P-h diagram of the proposed solar-driven ejector-compression system.

centres for district heating networks; and finally, to reduce system overall carbon footprint.

2. System description

2.1. Configuration

The system consists of a compound PV/T waste heat-driven ejector-heat pump for simultaneous heating and cooling purposes, using waste heat for system performance enhancement. It comprises a compressor, flash tank, ejector, two expansion valves (high- and low-pressure) and several heat exchangers: condenser, evaporative-condenser, generator, PV/T waste heat exchangers, and evaporator heat exchangers, as shown in Fig. 1.

The system is designed for three functions. The PV/T operating temperature is decreased, and the generated electric power is maximised. This waste heat is used as the generator heat source, acting with the vapour generated in an evaporative-condenser as the ejector driving force. The temperature reaches more than 65°C, so the saturation pressure ranges from 16.6 bar to 23.4 bar for all studied refrigerants, and it is within the recommended range as recommended in several studies (Li et al., 2018; Xu et al., 2018a). In the PVT system, the heat storage tank is employed in the absence of sun (Xu et al., 2018b) However, we overcome this issue in the current configuration with a condenser waste heat exchanger instead of hot tank storage. This component actuates according to the available solar intensity (Al-Sayyab et al., 2021). The second function is to absorb the data centre waste heat generated and maintain the indoor air conditions in the ASHRAE comfort zone. Finally, this heat is upgraded to the compressor functional temperature levels, specifically for district heating.

The novel system arrangement has excellent potential for energy-saving and carbon footprint reduction using low global warming refrigerants. Another novelty is the ejector arrangement, which saves electricity by removing the pump and reducing the compressor pressure ratio. Moreover, the auxiliary heat exchanger uses the condenser waste heat to compensate for the absence of solar intensity (overcast day conditions).

2.2. Low global warming refrigerants

Hydrofluorocarbons (HFCs) are worldwide used as working fluids in air-conditioning and refrigeration applications, but they are being phased out under the Montreal Protocol as potent greenhouse gases. One of the most used HFCs is R134a, which has 1430 times the impact of carbon dioxide in global warming potential (GWP). In October 2016, the parties decided to accelerate their schedule to phase down HFCs to recognise the potential benefits to the Earth. Signing developed countries have reduced their HFCs consumption and will completely phase out by 2050 (United Nations Environment Programme (UNEP), 2019).

In the current study, eleven environmentally friendly refrigerants are considered, from different safety groups with very low GWP, Table 1, to choose the most appropriate low GWP refrigerant for the proposed system.

3. Methodology

3.1. System modelling

The energy-exergy performance and environmental analysis of the current system are carried out, as shown in Fig. 2. The Engineering Equation Solver (EES) software (Klein, 2020), together with REFPROP (NIST Reference Fluid Thermodynamic and Transport Properties Database (REFPROP): Version 10, 2018), for mixture properties, are used to model the proposed system and introduce all the considered assumptions, boundary conditions and inputs. Moreover, the model also includes all the required equations to evaluate the performance with different working fluids, the influence of solar intensity, real climate data, and PV/T and ejector sub-models.

3.2. Boundary conditions and assumptions

The ambient air temperatures and hourly solar intensity are based on Valencia (Spain) real data (VISUAL CROSSING, 2021). These are considered as the input parameters to determine the hourly system performance for the data centre cooling system. A constant data centre cooling load of 90 kW is simulated for all the operating conditions. The refrigerant leaving the condenser is assumed as wet vapour; meanwhile, an ideal flash tank is simulated (saturated vapour from the upper part and saturated liquid from the bottom). The pressure drops and heat transfer to the surrounding through the connection pipes and compressor are neglected. Table 2 summarises the main assumptions and boundary conditions.

3.3. Model equations

The source of thermodynamic inefficiencies, irreversibilities of the components, and carbon footprint are calculated to identify the most suitable refrigerant. Henceforth, an energetic-exergetic-environmental (3E) system evaluation is carried out.

3.3.1. Energetic and operational model

The compressor power consumption can be obtained using Eq. (1).

$$\dot{W}_c = \frac{\eta_{em}}{\eta_{is}} \dot{m}_r \left(\overline{h}_{c,out} - h_{c,in}\right) \quad (1)$$

The refrigerant mass flow rate delivered by the compressor is obtained by Eq. (2).

Table 1
Thermophysical properties of the alternative low-GWP refrigerants and the reference R134a (ASHRAE, 2019; Klein, 2020).

Refrigerants	Molecular weight(g mol^{-1})	T_{crit} (°C)	P_{crit} (MPa)	NBP(°C)	ρ(kg m^{-3})	h_{fg}(kJ kg^{-1})	ODP	GWP_{100}	Safety class ASHRAE
R134a	102.03	101.0	40.59	-26.09	5.258	217.0	0	1430	A1
R450A	108.70	104.5	38.22	-23.39	5.522	204.2	0	605	A1
R513A	108.40	94.91	36.47	-29.52	5.679	194.8	0	631	A1
R515A	118.70	108.7	35.66	-18.74	5.939	188.0	0	393	A1
R515B	117.48	108.0	35.63	-18.80	5.877	190.0	0	299	A1
R516A	102.58	97.30	36.45	-29.40	5.375	202.8	0	142	A2L
R152a	66.05	113.3	45.20	-24.05	3.376	329.9	0	124	A2
R444A	96.70	106.0	39.38	-35.70	4.937	234.2	0	92	A2L
R1234ze(E)	114.0	109.4	36.32	-19.28	5.706	195.6	0	7	A2L
R1234yf	114.0	94.70	33.82	-29.49	5.981	180.2	0	4	A2L
R290	44.10	96.68	42.47	-42.10	2.417	425.8	0	3	A3
R1243zf	96.05	103.8	35.18	-25.43	4.946	217.2	0	1	A2L

*At a pressure of 1.01325 bar.

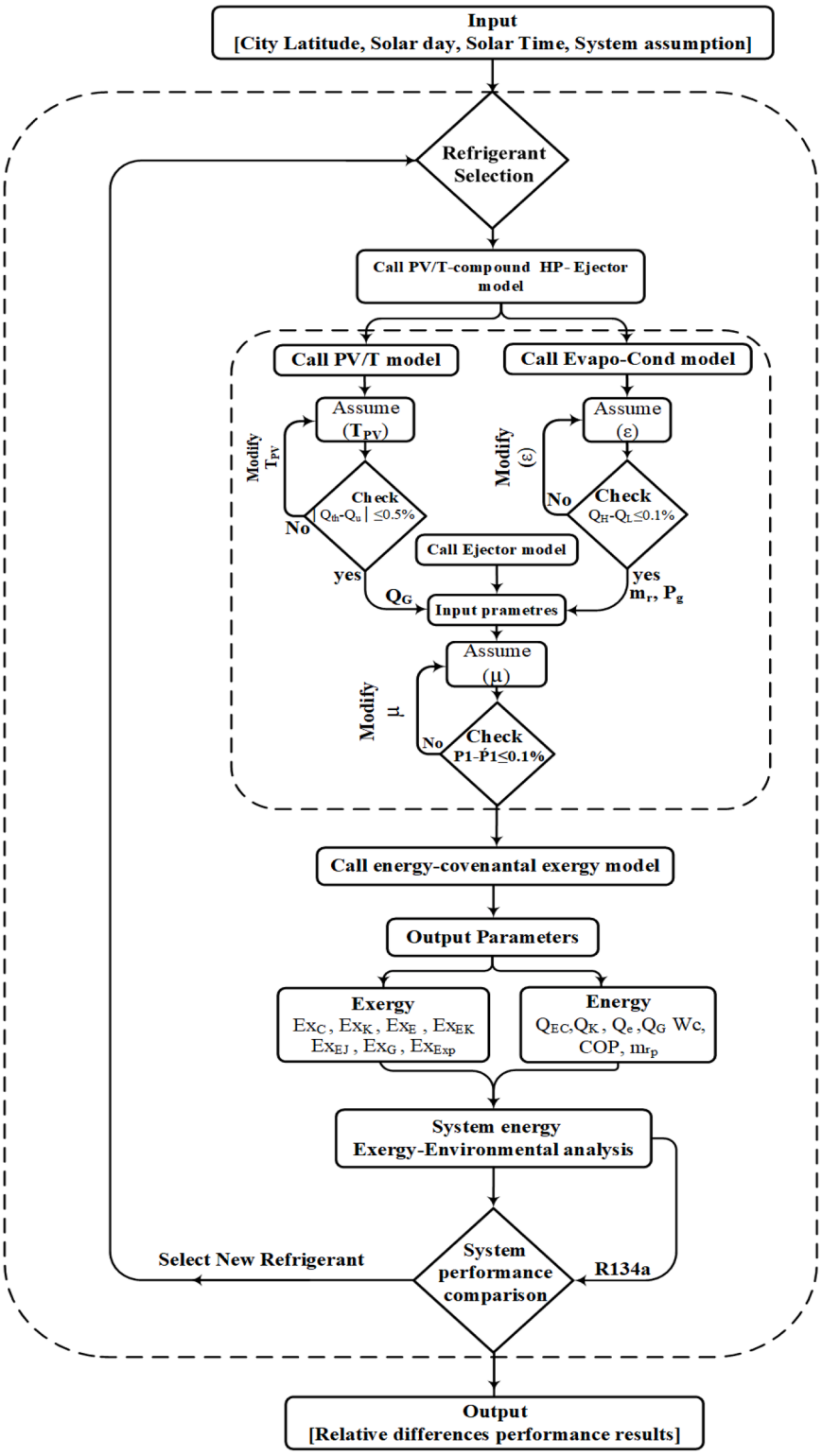

Fig. 2. Flow diagram for the methodology.

$$\dot{m}_r = \frac{\eta_v V_{DS} rpm}{v} \tag{2}$$

The compressor volumetric efficiency and isentropic efficiency are calculated as follows Bai et al., 2019; Chen and Yu, 2017b), Eq. (3) and ((4).

$$\eta_v = 0.9 - 0.035\frac{p_d}{p_s} \tag{3}$$

$$\eta_{is} = 0.976695 - 0.0366432\frac{p_d}{p_s} + 0.0013378\left(\frac{p_d}{p_s}\right)^2 \tag{4}$$

Heating capacity can be obtained from Eq. (5).

$$\dot{Q}_k = \dot{m}_r\left(h_{k,out} - h_{k,in}\right) \tag{5}$$

The cooling load is assumed to be constant for the data centre, so the

Table 2
Assumptions and boundary conditions.

Parameters	Assumed value
ΔT_{ew}	5 K (Yan et al., 2018)
ΔT_{Kw}	20 K
PV/T area	1.65*1.3*350 m^2
Compressor rotational speed	2900 rpm
V_{DS}	0.001936 m^3 (Al-Sayyab et al., 2021)
$\eta_{n;}\eta_{D;}\ \eta_{mx}$	0.85 (Sun, 1997)
η_{em}	0.88 (Al-Sayyab et al., 2021)
LK	3% of refrigerant charge (Makhnatch and Khodabandeh, 2014)
α,n	15 years (Mansuriya et al., 2020)
RT	Valencia: 5040 hours
β	Valencia: 265.4 g CO_2-eq kWh^{-1} (The European Environment Agency, 2018)
γ_{Eco_2}	968 g kWh^{-1} (Wang et al., 2010)
γ_{Fco_2}	220 g kWh^{-1} (Wang et al., 2010)

refrigerant mass flow rate can be calculated through a heat balance in the evaporator, Eq. (6).

$$\dot{m}_e = \frac{\dot{Q}_e}{(h_{e,in} - h_{e,out})} \tag{6}$$

The evaporative-condenser effectiveness can be evaluated by Eq. (7).

$$\varepsilon_{ek} = \frac{h_{in,h} - h_{out,h}}{h_{in,h} - h_{in,l}} \tag{7}$$

The constant mixing area model is adopted to obtain its thermodynamic, in the ejector analysis, performance suggested, as proved by previous investigations (Bai et al., 2019; Cui et al., 2020; Pan et al., 2020). The most critical factor is the entrainment ratio, which can be calculated through Eq. (8).

$$\mu = \frac{\dot{m}_s}{\dot{m}_p} \tag{8}$$

The primary refrigerant exit velocity from the nozzle is based on the conservation law, and it can be obtained using Eq. (9).

$$\omega_{pn} = \sqrt{2\left(h_{(pn)i} - h_{(pn)ea}\right)} \tag{9}$$

In the same way, the secondary refrigerant exit velocity can be obtained following Eq. (10).

$$\omega_{sn} = \sqrt{2\left(h_{(sn)i} - h_{(sn)ea}\right)} \tag{10}$$

The refrigerant velocity and enthalpy of the mixing chamber can be obtained by applying momentum and energy conservation equations on the ejector mixing chamber, Eq. (11) and Eq. (12), respectively.

$$\omega_m = \sqrt{\eta_m}\left(\omega_{sn}\left(\frac{\mu}{1+\mu}\right) + \omega_{pn}\left(\frac{1}{1+\mu}\right)\right) \tag{11}$$

$$h_m = \frac{1}{1+\mu}\left(h_{(pn)ea} + \frac{\omega_{pn}{}^2}{2}\right) + \frac{\mu}{1+\mu}\left(h_{(sn)ea} + \frac{\omega_{sn}{}^2}{2}\right) - \frac{\omega_m{}^2}{2} \tag{12}$$

For the diffuser suction, the outlet enthalpy can be obtained from Eq. (13).

$$h_{d,ea} = h_m + \frac{\omega_m{}^2}{2} \tag{13}$$

The system coefficient of performance in cooling mode (COP_C) and in heating mode (COP_H) results from Eq. (14) and Eq. (15), respectively.

$$COP_C = \frac{\dot{Q}_e}{\dot{W}_c} \tag{14}$$

Table 3
Exergy destruction rate equations for proposed system components (Al-Sayyab and Abdulwahid, 2019) (T.J.Kotas, 1985).

Component	Exergy Equation
Compressor	$\dot{E}X_{Des,C} = \dot{E}X_{in} - \dot{E}X_{out} - \dot{w}_c$
Condenser	$\dot{E}X_{Des,K} = (\dot{E}X_{in} - \dot{E}X_{out})_r + (\dot{E}X_{in} - \dot{E}X_{out})_w$
Evaporative-Condenser	$\dot{E}X_{Des,ek} = (\dot{E}X_{in} - \dot{E}X_{out})_{rl} + (\dot{E}X_{in} - \dot{E}X_{out})_{rh}$
Generator	$\dot{E}X_{Des,g} = (\dot{E}X_{in} - \dot{E}X_{out})_r + (\dot{E}X_{in} - \dot{E}X_{out})_w$
Ejector	$\dot{E}X_{Des,ej} = \dot{E}X_{in} - \dot{E}X_{out}$
Expansion valve	$\dot{E}X_{Des,exp} = \dot{E}X_{in} - \dot{E}X_{out}$
Evaporator	$\dot{E}X_{Des,e} = (\dot{E}X_{in} - \dot{E}X_{out})_r + (\dot{E}X_{in} - \dot{E}X_{out})_w$

$$COP_H = \frac{\dot{Q}_k}{\dot{W}_c} \tag{15}$$

3.3.1.1. Exergetic model. The exergy analysis indicates where the system efficiency can be improved. It is a way to determine the location, magnitude, and source of irreversibility. It evaluates the irreversibility occurring in the components of thermodynamic systems. A control volume is adopted without accounting for the PV/T panels and data centre room. Ambient temperature and pressure are taken as dead state conditions. The general exergy balance equation can be written as follows (T.J.Kotas, 1985).

$$0 = \left(1 - \frac{T_0}{T_b}\right)Q - \dot{w} + \dot{E}X_{in} - \dot{E}X_{out} - \dot{E}X_{DS} \tag{16}$$

$$\dot{E}X = \dot{m}(h - h_0 - T_0(s - s_0)) \tag{17}$$

The exergy destruction rate for each component can be listed in Table 3. Also, the total exergy destruction is the summation of all components follows Eq. (18).

$$\dot{E}X_{Des,t} = \dot{E}X_{Des,c} + \dot{E}X_{Des,k} + \dot{E}X_{Des,ek} + \dot{E}X_{Des,g} + \dot{E}X_{Des,ej} + \dot{E}X_{Des,exp} + \dot{E}X_{Des,e} \tag{18}$$

The exergy efficiency is as presented in Eq. (19).

$$\eta_{II} = 1 - \frac{\dot{E}X_{Des,t}}{\dot{E}X_{in}} \tag{19}$$

3.3.1.2. Environmental model. The current system presents a new arrangement of simultaneous cooling for data center and district heating by waste heat from different sources (PV/T and data center). Meanwhile, the electricity generated by the PV/T system is used to operate the heat pump. All these factors produce an immediate benefit in CO_2-eq emissions reduction.

The CO_2-eq emission reduction can be obtained employing Eq. (20) (Deymi-Dashtebayaz and Valipour-Namanlo, 2019; Wang et al., 2010), quantified by the natural gas saving.

$$\dot{m}_{fCO_2} = \gamma_{FCO_2}\dot{Q}_k\ RT \tag{20}$$

The CO_2-eq emission reduction quantified by electricity saving owing to system enhancement can be obtained by Eq. (21) (Wang et al., 2010).

$$\dot{m}_{el,CO2} = \gamma_{el,CO_2}\ (\dot{W}_{HP} - \dot{W}_{EHP})RT \tag{21}$$

The CO_2-eq emission reduction due to PVT generated electricity utilisation can be obtained by Eq. (22)

$$\dot{m}_{PVT,CO2} = \gamma_{el,CO_2}\dot{E}_{PVT} \tag{22}$$

Besides the possible energetic benefits, it is essential to determine the system carbon footprint. The Total Equivalent Warming Impact (TEWI) metric is appropriate for determining various refrigerants in heat

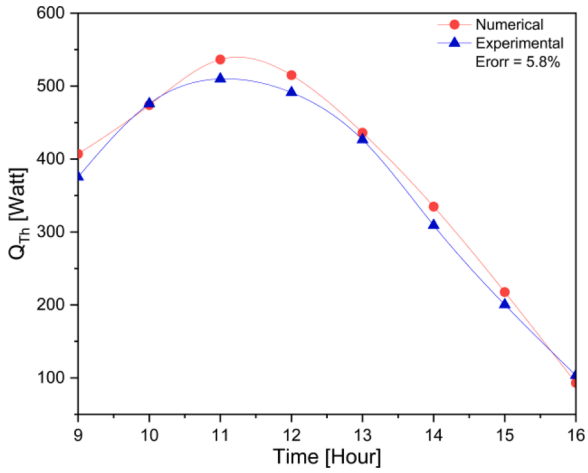

Fig. 3. PVT model validation.

pumps. The components of the TEWI are 1) direct emissions from accidental refrigerant leakages and 2) indirect emissions from fossil fuel burning for generating electricity. As a result, TEWI is calculated through Eq. (23) (Makhnatch and Khodabandeh, 2014).

$$TEWI = (GWP\ LK\ \alpha) + (EC\ \beta\ RT\ \alpha) \quad (23)$$

The models mentioned in Duffie et al. (2013), Shaker Al-Sayyab et al. (2019), Bahaidarah et al. (2013), and Tiwari et al. (2006) are used to evaluate the effect of hourly variations of solar intensity and ambient temperatures on PV/T performance.

4. Results and discussion

4.1. Simulation model validations

There are two models in the current study that have been validated, PVT and ejector.

Firstly, the experimental data of Bahaidarah et al. (2013) is used to validate the PVT model for different solar irradiance. Therefore, the operating conditions and PVT panel characteristics have been retrieved from their work. Fig. 3 shows the PVT waste heat recovered, and it can be seen that the PVT model agrees with the experimental results with an average error of 5.8%.

The second validation is the ejector-vapour refrigeration cycle combination. Zhao et al. (2019) and Sarkar (2009) results are used to checking the mentioned model at different conditions and refrigerants. The results obtained from this validation are compared in Tables 4 and 5 compared with Zhao et al. (2019) using R290. Fig. 4 includes the comparison with Sarkar (2009) at different condensing temperatures using R600a. Based on the minimum deviation observed, the current ejector model shows a good agreement with the selected works.

4.2. Energy analysis

4.2.1. Effect of solar intensity on system performance

Fig. 5 illustrates the effect of solar intensity variation for 15 January on system performance operating with different refrigerants for constant condensing and evaporating temperatures and data centre cooling capacity.

Fig. 5.a evidence that the compressor specific work decreases as solar intensity increases, reaching the lowest value at the highest solar intensity period (01:00 PM). This reduction is because the system uses the maximum PV/T waste heat as the ejector driving force. As a result, the generator temperature increases, the ejector pressure is augmented, and the compressor pressure ratio is reduced, Fig. 5.b. A similar conclusion can be obtained regarding the refrigerant mass flow rate, Fig. 5.c. The superheating degree and the decrease of compressor pressure ratio compensate for the increase in the refrigerant mass flow rate; therefore, the compressor power consumption does not significantly change with the solar intensity variation during the day Fig. 5.d. The evolution of condenser heating capacity is contrary to the specific compression work, which gradually increases as the solar intensity increases, reaching a maximum at the period of highest solar intensity (01:00 PM), Fig. 5.e.

The system using R515B results in the lowest compressor power

Table 5
Current ejector model result comparison with Zhao et al. (2019).

Result	Zhao et al.	Ejector model of current study	Error %
COP	1.91	1.99	4.19
μ	0.3478	0.3478	0

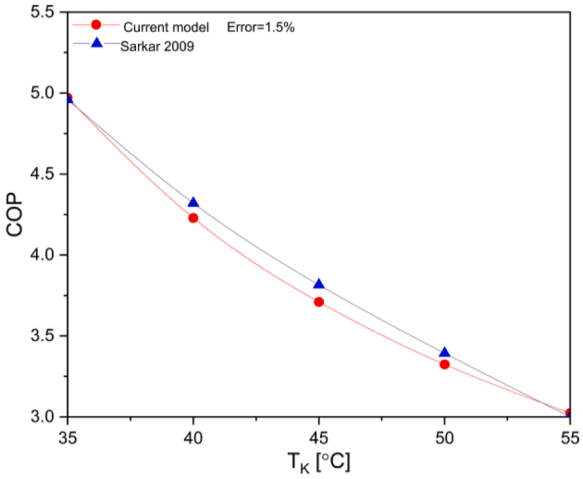

Fig. 4. Ejector model validation

Table 4
State points of current ejector model result comparison with Zhao et al. (2019).

Point	h (kJ kg^{-1})			s (kJ kg^{-1})			T (°C)		
	Zhao et al.	Current study	Error (%)	Zhao et al.	Current study	Error (%)	Zhao et al.	Current study	Error (°C)
1	556.5	556.5	0	2.46	2.45	-0.33	-18.66	-18.02	0.64
2	686.7	681.4	-0.77	2.56	2.55	-0.59	73.01	70.58	-2.43
3	307.8	307.8	0	1.36	1.36	+0.15	40	40	0
4	307.8	307.8	0	1.41	1.42	+0.14	-10	-10	0
5	463.3	463.3	0	2.00	2.00	+0.15	-10	-10	0
6	175.2	175.2	0	0.91	0.91	+0.18	-10	-10	0
7	563.4	563.4	0	2.38	2.38	+0.17	-10	-10	0
N	532.2	532.2	0.43	2.40	2.41	+0.29	-33	-33	0
8	175.2	175.2	0	0.92	0.92	+0.02	-33	-33	0
9	536.7	536.7	0	2.42	2.43	+0.21	-33	-33	0
M	543.6	540.0	-0.66	2.45	2.44	-0.45	-28.42	-30.78	-2.36

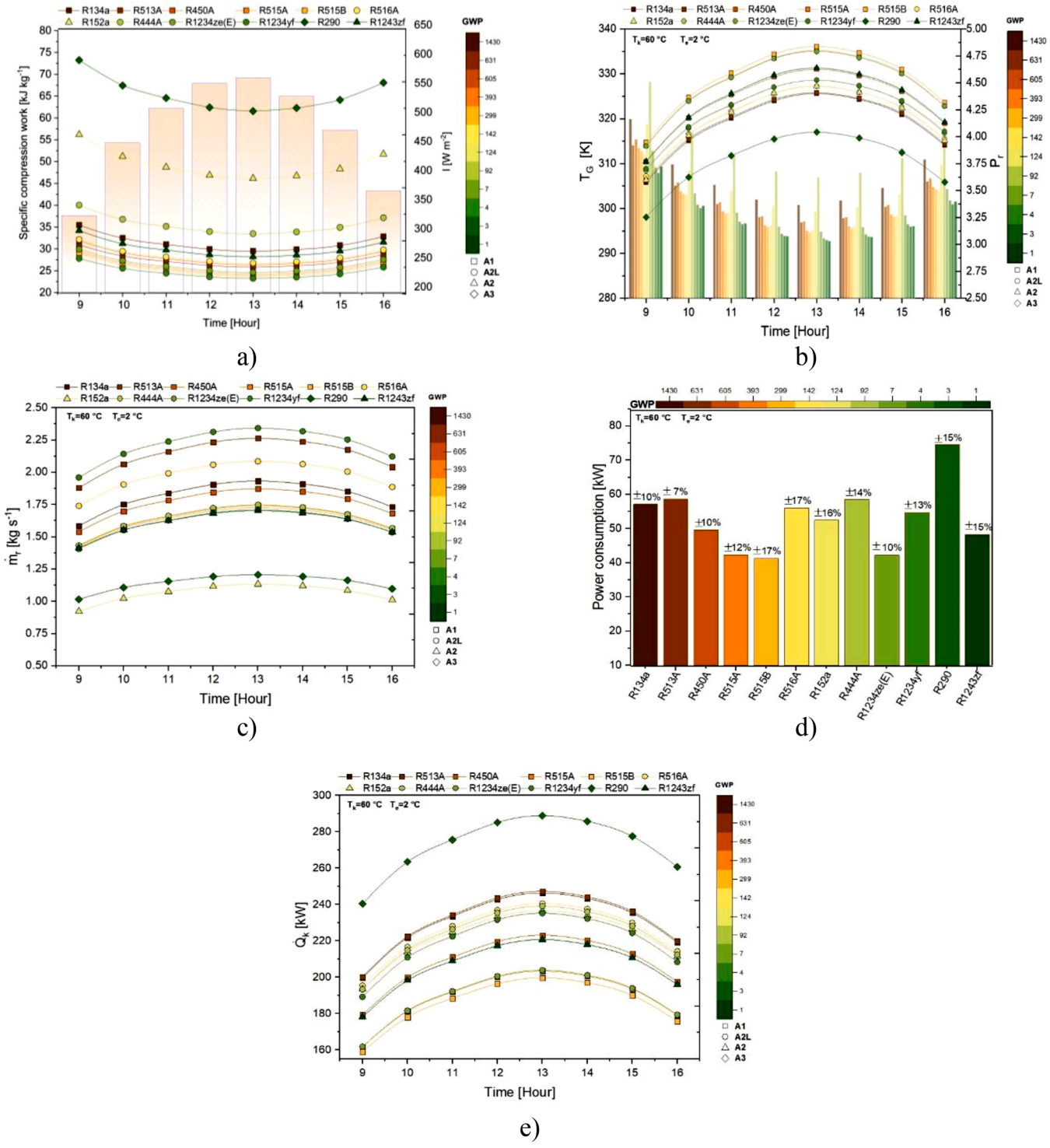

Fig. 5. Effect of solar time variation on a) compressor specific work, b) pressure ratio, c) refrigerant mass flow rate, d) power consumption, e) heating capacity

consumption. On the contrary, using R290, the system depicts the highest consumption despite the low refrigerant mass flow rate that does not compensate for the highest specific compression work. Then, R290 has the highest condenser heating capacity, followed by R513A, owing to R290 has the highest latent heat of vaporisation; meanwhile, R513A has the highest vapour density with the moderate latent heat of vaporisation (Table. 1)

Fig. 6.a and Fig. 6.b show the effect of solar intensity variation on the system performance in cooling (COP_C) and heating (COP_H) mode. The system performance is benefitted from higher solar intensity because of the influence of solar intensity on the compressor pressure ratio, which is reduced. Hence, the reduction of compressor specific work and the increase of heating and cooling capacity enhance both modes energy performance. R515B shows the highest system performance in cooling and heating modes, followed by R1234ze(E) and R515A. However, the system using R290 presents the worst performance in both modes due to its highest power consumption owing to R290 has the highest latent heat of vaporisation requires more heat (the current system used waste heat to drive the ejector that gives compressor pressure ratio reduction enhancement so as less compressor work).

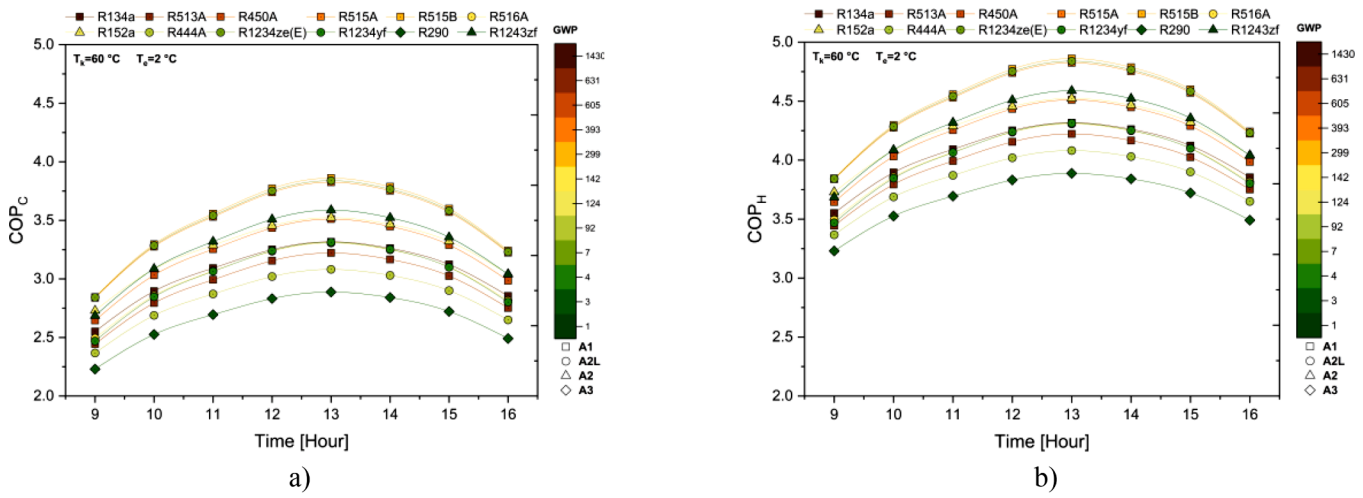

Fig. 6. Effect of solar time variation on the system a) COP_C, and b) COP_H

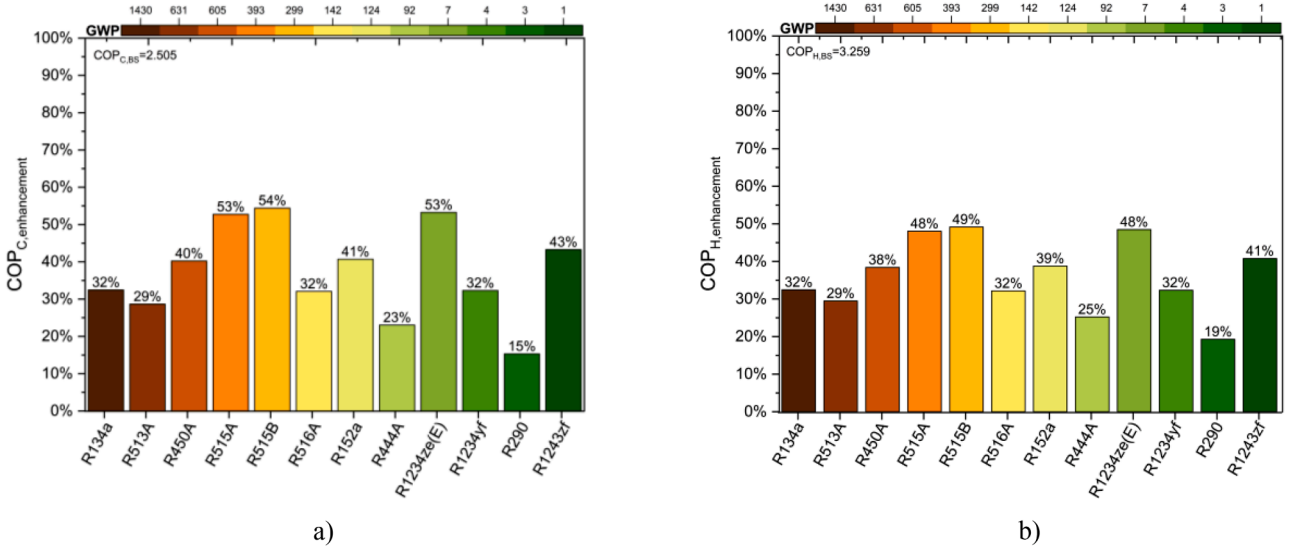

Fig. 7. Performance improvement caused by different refrigerants: a) COP_C, and b) COP_H.

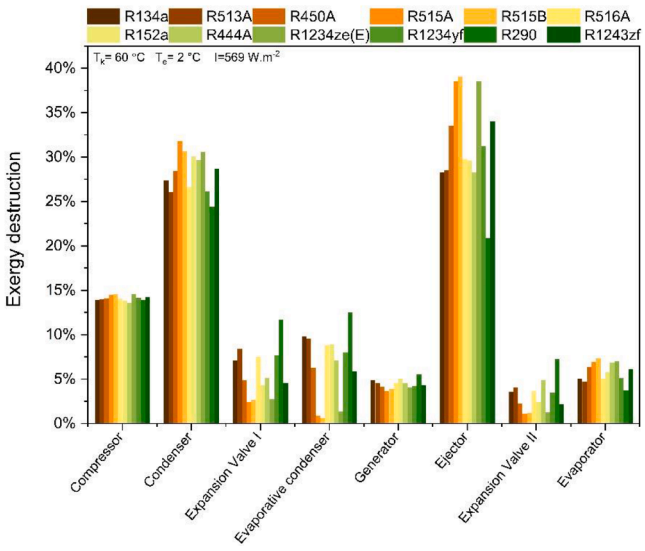

Fig. 8. Exergy destruction in each component

Finally, Fig. 7 shows that the proposed system provides a COP_C and COP_H improvement with all refrigerants analysed compared to the proposed system with a conventional heat pump due to compressor work reduction resulting from the compressor-ejector combination. The system using R515B has a COP_C improvement of 54%, followed by R515A and R1234ze(E), with 53% Fig. 7.a, meanwhile, in heating mode, the system using R515B shows a COP_H enhancement by 49%, close to R515A and R1234ze(E), with 48%, Fig. 7.b.

4.3. Exergy analysis

This section analyses the system exergy performance with fixed condensing and evaporating temperatures and solar intensity, Fig. 8. It is stated that the ejector represents the largest source of exergy destruction of the whole system exergy destruction for most refrigerants, followed by the condenser and then the compressor. The ejector has varied irreversibility sources, such as the nozzles flow friction irreversibility, two streams mixing irreversibility (the primary and the secondary flow), and compression shock waves irreversibility (Li et al., 2018). For the best refrigerant in terms of energy performance. The R515B ejector exergy destruction represents 39% of the total system exergy destruction, followed by the condenser, 31%, and compressor, 14%. Meanwhile, the

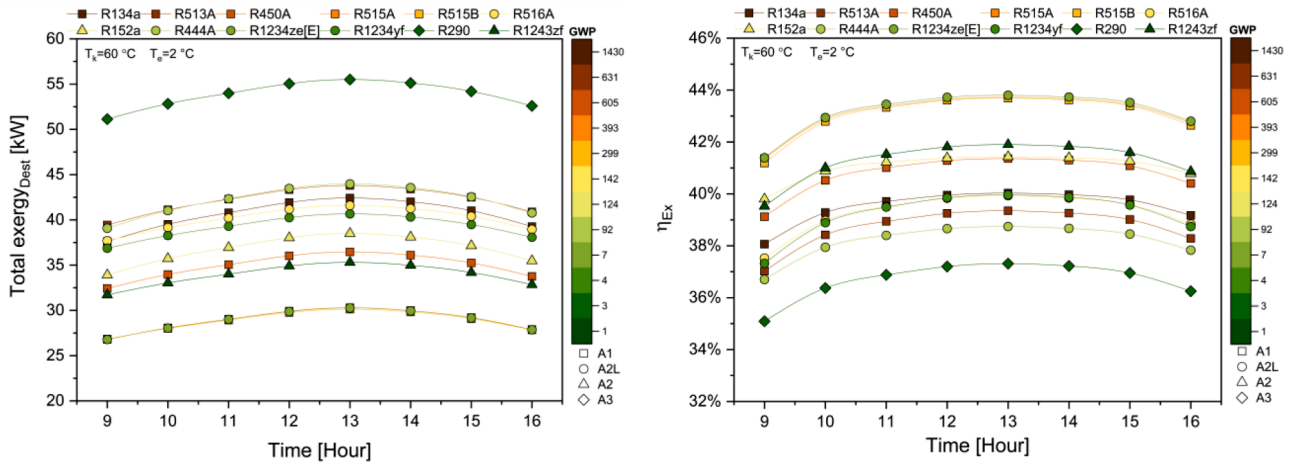

Fig. 9. Effect of solar time variation on exergetic parameters

evaporative- condenser and the second expansion valve comprise the lowest exergy destruction percentage, 1%.

Fig. 9 shows the effect of the solar intensity variation for 15 January on the total exergy destruction rates. The total exergy destruction is directly proportional to the solar intensity due to increased exergy input (solar intensity). The high generator temperature will increase the refrigerant mass flow rate and the heating capacity, increasing the entertainment ratio and directly influencing system irreversibility (Pridasawas and Lundqvist, 2004) (at the condenser, generator, and evaporative condenser). In other words, it increases the amount of irreversibility in all components.

Fig. 9 also shows the effect of the solar intensity variation on the system exergy efficiency at fixed condensing and evaporating temperatures. The exergy efficiency increases gradually during sunrise and reaches the highest value at midday (the highest solar intensity), then it slightly falls until sunset. Thus, the exergy efficiency increases as the solar intensity increases. This trend is mainly determined by the decrease of exergy destruction in both the compressor and generator, owing to the pressure ratio decrease and heat transfer at lower temperature differences.

Meanwhile, the system input exergy increased due to the waste heat recovered from PVT. Besides, the exergy gained by the water through the condenser (the system exergy output) exhibits a higher rise than destruction. All these factors contribute to an enhancement in the system exergy efficiency.

The system using R290 has the highest exergy destruction than the rest of the refrigerants at a constant solar intensity. The lowest exergy destruction is achieved using R515B, R515A and R1234ze(E). Similarly, the system using these refrigerants has the highest exergy efficiency because of the lowest exergy destruction. That means the system should be getting more attention for optimisation with R290.

4.4. Environmental analysis

As shown in Fig. 8, the proposed system provides remarkable GHG emissions reduction by different factors: 1) better efficiency of the data centre cooling system by reducing the power consumption, 2) renewable energy generated by the PV/T panels, and 3) use of the condenser waste heat for district heating.

The proposed system shows an energetic and exergetic performance improvement for all low GWP refrigerants analysed, leading to significant carbon footprint reduction. Compared with the most common cooling and heating methods in Spain (based on a chiller for data centre cooling and a natural gas boiler for heating), the proposed system can save more than half of the energy consumption. The system using R1234ze(E), R515B and R515A shows a comparable reduction of tCO_2-eq year^{-1} from lower compressor power consumption (indirect emissions) for data centre cooling. Meanwhile, there is an augmentation when using R290 due to the higher power consumption required. On the other hand, all the refrigerants investigated show a comparable reduction for the tCO_2-eq year^{-1} caused by the PV/T electric power. In the condenser waste heat recovery scenario, the R290 system shows the highest reduction of tCO_2-eq year^{-1} by the highest condenser heating capacity that causes the highest waste heat recovery, followed by the systems of R516A, R152a and R444A. Finally, R515B, R515A and R1234ze(E) show comparable promising values for a total reduction of

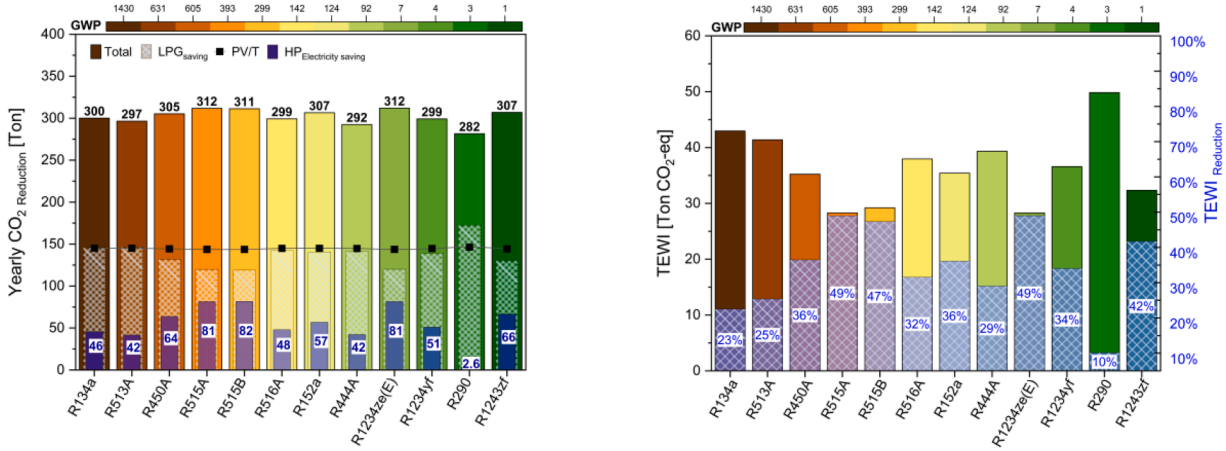

Fig. 10. Environmental performance with different refrigerants.

tCO_2-eq $year^{-1}$.

This section compares the TEWI of the proposed system with a simulated R134a traditional heat pump having the same refrigeration capacity to get a meaningful value of the TEWI and TEWI percentage reduction (Islam and Saha, 2020).

Fig. 10 illustrates the TEWI of the proposed system with all the refrigerants analysed. The system using R1234ze(E) and R515A shows the lowest TEWI, followed by R515B. Meanwhile, compared with the reference system using R134a, the proposed system shows a TEWI reduction ranged from 10% (R290) to 49% (R515A and R1234ze(E)).

5. Conclusions

We proposed a novel simultaneous data center cooling system with waste heat utilisation for a district heating system. Several future-proof technologies are combined, including PV/T, ejector-heat pump, and waste heat utilisation. This solution caused an overall system performance enhancement and remarked energy-saving and CO_2-eq emissions reduction.

For all investigated refrigerants, the novel system arrangement shows an overall system performance enhancement. The most significant improvement in the cooling mode performance occurs with R515B, having a 54% increase compared to the R134a reference system, followed by R515A and R1234ze(E). Meanwhile, in the heating mode, R515B shows a 49% system COP enhancement. In the exergetic analysis, the ejector shows the highest exergy destruction compared to the rest of the components, followed by the condenser and compressor. In comparison to the rest of the refrigerants, R290 shows the highest total system exergy destruction. On the other hand, the system of R515B show the lowest values for this parameter; for this reason, the R515B system shows the highest exergy efficiency.

Finally, to complete the multi-perspective analysis, it is worth mentioning that the novel system arrangement shows various CO_2-eq emission reduction sources. The reduction comes from the PV/T generated electricity utilisation. The most significant reductions are obtained by R515B, R515A and R1234ze(E), up to 49%.

Related to the developed work, there are multiple ways to continue it and make it more comprehensive. To highlight a few examples, these results could be used for carrying out a multi-objective optimisation of the system for the optimum refrigerant, or a detailed economic study of the proposed configuration could be added, so the 3E analysis becomes 4E. Besides, the system could be coupled to other residential, commercial, or industrial applications with heating or cooling excess or demand, implying other operational conditions and modifying the equations used for environmental or economic analysis.

Declaration of Competing Interest

We wish to confirm that there are no known conflicts of interest associated with this publication and there has been no significant financial support for this work that could have influenced its outcome.

Acknowledgments

Ali Khalid Shaker Al-Sayyab gratefully acknowledges the Southern Technical University in Iraq for the financial support to complete this work. Adrián Mota Babiloni acknowledges the postdoctoral contract “Juan de la Cierva-Incorporación 2019” of the Spanish State Research Agency (IJC2019-038997-I).

References

Al-Sayyab, A.K.S., Abdulwahid, M.A., 2019. Energy-exergy analysis of multistage refrigeration system and flash gas intercooler working with ozone-friendly alternative refrigerants to R134a. J. Adv. Res. Fluid Mech. Therm. Sci. 63, 188–198.

Al-Sayyab, A.K.S., Navarro-Esbrí, J., Soto-Francés, V.M., Mota-Babiloni, A., 2021. Conventional and advanced exergoeconomic analysis of a compound ejector-heat pump for simultaneous cooling and heating. Energies 14. https://doi.org/10.3390/en14123511.

Al-Sayyab, Ali Khalid Shaker, Mota-Babiloni, Adrián, Fernández, Adrián, E, J.N., 2021. Influence of the evaporating temperature on lower GWP refrigerants used in a compound waste heat-solar driven ejector- compression heat pump. In: Thermophysical Properties and Transfer Processes of Refrigerants Conference (TPTPR2021)At: Vicenza (Italy). https://doi.org/10.18462/iir.TPTPR.2021.2104.

ASHRAE, 2019. Standard 34, Designation and Safety Classification of Refrigerants.

Avgerinou, M., Bertoldi, P., Castellazzi, L., 2017. Trends in Data Centre Energy Consumption under the European Code of Conduct for. Data Centre Energy Efficiency. Energies 10. https://doi.org/10.3390/en10101470.

Bahaidarah, H., Subhan, A., Gandhidasan, P., Rehman, S., 2013. Performance evaluation of a PV (photovoltaic) module by back surface water cooling for hot climatic conditions. Energy 59, 445–453. https://doi.org/10.1016/j.energy.2013.07.050.

Bai, T., Yan, G., Yu, J., 2019. Thermodynamic assessment of a condenser outlet split ejector-based high temperature heat pump cycle using various low GWP refrigerants. Energy 179, 850–862. https://doi.org/10.1016/j.energy.2019.04.191 https://doi.org/https://doi.org/.

Bai, Y., Chow, T.T., Ménézo, C., Dupeyrat, P., 2012. Analysis of a hybrid PV/thermal solar-assisted heat pump system for sports center water heating application. Int. J. Photoenergy 2012. https://doi.org/10.1155/2012/265838.

Boumaraf, L., Haberschill, P., 2016. Performance of a solar -driven ejector refrigerating system using fluids with low ecological impact. Int. J. Energy, Environ. Econ. 24, 393–401.

Byrne, P., Ghoubali, R., 2019. Exergy analysis of heat pumps for simultaneous heating and cooling. Appl. Therm. Eng. 149, 414–424. https://doi.org/10.1016/j.applthermaleng.2018.12.069.

Chen, J., Yu, J., 2017a. Theoretical analysis on a new direct expansion solar assisted ejector-compression heat pump cycle for water heater. Sol. Energy 142, 299–307. https://doi.org/10.1016/j.solener.2016.12.043 https://doi.org/https://doi.org/.

Chen, J., Yu, J., 2017b. Theoretical analysis on a new direct expansion solar assisted ejector-compression heat pump cycle for water heater. Sol. Energy 142, 299–307. https://doi.org/10.1016/j.solener.2016.12.043.

Cui, Z., Qian, S., Yu, J., 2020. Performance assessment of an ejector enhanced dual temperature refrigeration cycle for domestic refrigerator application. Appl. Therm. Eng. 168, 114826 https://doi.org/10.1016/j.applthermaleng.2019.114826 https://doi.org/https://doi.org/.

Davies, G.F., Maidment, G.G., Tozer, R.M., 2016. Using data centres for combined heating and cooling: an investigation for London. Appl. Therm. Eng. 94, 296–304. https://doi.org/10.1016/j.applthermaleng.2015.09.111.

Deymi-Dashtebayaz, M., Valipour-Namanlo, S., 2019. Thermoeconomic and environmental feasibility of waste heat recovery of a data center using air source heat pump. J. Clean. Prod. 219, 117–126. https://doi.org/10.1016/j.jclepro.2019.02.061 https://doi.org/https://doi.org/.

EEA, 2020. Fluorinated greenhouse gases 2020.

European Commission, 2015. Ecodesign Preparatory Study on Enterprise Servers and Data Equipment.

Fu, H.D., Pei, G., Ji, J., Long, H., Zhang, T., Chow, T.T., 2012. Experimental study of a photovoltaic solar-assisted heat-pump/heat-pipe system. Appl. Therm. Eng. 40, 343–350. https://doi.org/10.1016/j.applthermaleng.2012.02.036.

GeSI. SMART 2020, 2008. enabling the low carbon economy in the information age. Ecography. https://doi.org/10.1111/j.0906-7590.2007.04873.x.

GlobalABC/IEA/UNEP, 2020. GlobalABC Roadmap for Buildings and Construction 2020-2050.

Hazi, A., Hazi, G., 2014. Comparative study of indirect photovoltaic thermal solar-assisted heat pump systems for industrial applications. Appl. Therm. Eng. 70, 90–99. https://doi.org/10.1016/j.applthermaleng.2014.04.051.

He, Z., Ding, T., Liu, Y., Li, Z., 2018. Analysis of a district heating system using waste heat in a distributed cooling data center. Appl. Therm. Eng. 141, 1131–1140. https://doi.org/10.1016/j.applthermaleng.2018.06.036.

Huang, Z., Zhao, H., Yu, Z., Han, J., 2018. Simulation and optimization of a R744 two-temperature supermarket refrigeration system with an ejector. Int. J. Refrig. 90, 73–82. https://doi.org/10.1016/j.ijrefrig.2018.04.007.

IEA, 2018. The Future of Cooling: opportunities for energy-efficient air conditioning. Futur. Cool. Oppor. energy-efficient air Cond. 92.

IEA, World Energy Outlook 2019, IEA, Paris, 2019.

Islam, M.A., Saha, B.B., 2020. TEWI Assessment of Conventional and Solar Powered Cooling Systems BT - Solar Energy: Systems, Challenges, and Opportunities. Springer Singapore, Singapore, pp. 147–177. https://doi.org/10.1007/978-981-15-0675-8_9 in: Tyagi, H., Chakraborty, P.R., Powar, S., Agarwal, A.K. (Eds.).

Duffie, John A., B, W.A., 2013. Solar Engineering of Thermal Processes, 4Th ed. Wiley. Wiley. https://doi.org/10.1119/1.14178.

Khalid Shaker Al-Sayyab, A., Mota-Babiloni, A., Navarro-Esbrí, J., 2021. Novel compound waste heat-solar driven ejector-compression heat pump for simultaneous cooling and heating using environmentally friendly refrigerants. Energy Convers. Manag. 228, 113703 https://doi.org/10.1016/j.enconman.2020.113703 https://doi.org/https://doi.org/.

Klein, S., 2020. Engineering Equation Solver (EES) V10.2. Fchart software, Madison, USA.

Li, F., Chang, Z., Li, X., Tian, Q., 2018. Energy and exergy analyses of a solar-driven ejector-cascade heat pump cycle. Energy 165, 419–431. https://doi.org/10.1016/j.energy.2018.09.173 https://doi.org/https://doi.org/.

Makhnatch, P., Khodabandeh, R., 2014. The role of environmental metrics (GWP, TEWI, LCCP) in the selection of low GWP refrigerant. Energy Procedia 61, 2460–2463. https://doi.org/10.1016/j.egypro.2014.12.023.

Mansuriya, K., Patel, V.K., Raja, B.D., Mudgal, A., 2020. Assessment of liquid desiccant dehumidification aided vapor-compression refrigeration system based on thermo-economic approach. Appl. Therm. Eng. 164, 114542 https://doi.org/10.1016/j.applthermaleng.2019.114542 https://doi.org/https://doi.org/.

Mota-Babiloni, A., Makhnatch, P., Khodabandeh, R., 2017. Recent investigations in HFCs substitution with lower GWP synthetic alternatives: Focus on energetic performance and environmental impact. Int. J. Refrig. https://doi.org/10.1016/j.ijrefrig.2017.06.026.

Mukaffi, A.R.I., Arief, R.S., Hendradjit, W., Romadhon, R., 2017. Optimization of cooling system for data center case study: PAU ITB Data Center. Procedia Eng. 170, 552–557. https://doi.org/10.1016/j.proeng.2017.03.088.

NIST Reference Fluid Thermodynamic and Transport Properties Database (REFPROP): Version 10, 2018.

OECD /IEA, 2018. World Energy Model. World Energy Outlook 82.

Pan, M., Bian, X., Zhu, Y., Liang, Y., Lu, F., Xiao, G., 2020. Thermodynamic analysis of a combined supercritical CO2 and ejector expansion refrigeration cycle for engine waste heat recovery. Energy Convers. Manag. 224, 113373 https://doi.org/10.1016/j.enconman.2020.113373 https://doi.org/https://doi.org/.

Payerle, G., Team, R.C., Payerle, G., D, S., Dolnicar, S., Chapple, A., Pastuszak, A.W., Wang, R., 2015. Report to Congress on Server and Data Center Energy Efficiency public law 109-431. Public law 109. Ann. Tour. Res.

Pridasawas, W., Lundqvist, P., 2004. An exergy analysis of a solar-driven ejector refrigeration system. Sol. Energy 76, 369–379. https://doi.org/10.1016/j.solener.2003.11.004.

Sarkar, J., 2009. Performance characteristics of natural-refrigerants- based ejector expansion refrigeration cycles. Proc. Inst. Mech. Eng. Part A J. Power Energy 223, 543–550. https://doi.org/10.1243/09576509JPE753.

Shaker Al-Sayyab, A.K., Al Tmari, Z.Y., Taher, M.K., 2019. Theoretical and experimental investigation of photovoltaic cell performance, with optimum tilted angle: Basra city case study. Case Stud. Therm. Eng. 14, 100421 https://doi.org/10.1016/j.csite.2019.100421.

Sheme, E., Holmbacka, S., Lafond, S., Lučanin, D., Frashëri, N., 2018. Feasibility of using renewable energy to supply data centers in 60° north latitude. Sustain. Comput. Informatics Syst. 17, 96–106. https://doi.org/10.1016/j.suscom.2017.10.017.

SOLARGIS, 2019. global solar atlas [WWW Document]. URL https://globalsolaratlas.info/.

Sun, D.W., 1997. Solar powered combined ejector-vapour compression cycle for air conditioning and refrigeration. Energy Convers. Manag. 38, 479–491. https://doi.org/10.1016/S0196-8904(96)00063-5.

Kotas, T.J., 1985. The Exergy Method of Thermal Plant Analysis. Elsevier. https://doi.org/10.1016/C2013-0-00894-8.

The European Environment Agency, 2018. CO2 emission intensity [WWW Document]. URL https://www.eea.europa.eu/data-and-maps/daviz/co2-emission-intensity-5/download.table.

Tiwari, A., Sodha, M.S., 2006. Performance evaluation of solar PV/T system: An experimental validation. Sol. Energy 80, 751–759. https://doi.org/10.1016/j.solener.2005.07.006.

United Nations Environment Programme (UNEP), 2019. Handbook for the Montreal Protocol on Substances that Delete the Ozone Layer, 13th Ed. ISBN: 978-9966-076-59-5.

VISUAL CROSSING, 2021. Wather Data [WWW Document]. URL https://www.visualcrossing.com/weather-history/Valencia%2CSpain.

Wang, J., Zhai, Z.(John), Jing, Y., Zhang, C., 2010. Particle swarm optimization for redundant building cooling heating and power system. Appl. Energy 87, 3668–3679. https://doi.org/10.1016/j.apenergy.2010.06.021 https://doi.org/https://doi.org/.

Xu, Y., Jiang, N., Han, X., Han, W., Mao, N., Chen, G., 2018a. Performance evaluation and energy-saving potential comparison of a heat-powered novel compression-enhanced ejector refrigeration cycle with an economizer. Appl. Therm. Eng. 130, 1568–1579. https://doi.org/10.1016/j.applthermaleng.2017.11.106.

Xu, Y., Jiang, N., Wang, Q., Mao, N., Chen, G., Gao, Z., 2018b. Refrigerant evaluation and performance comparison for a novel hybrid solar-assisted ejection-compression refrigeration cycle. Sol. Energy 160, 344–352. https://doi.org/10.1016/j.solener.2017.12.030 https://doi.org/https://doi.org/.

Xu, Y., Wang, C., Jiang, N., Song, M., Wang, Q., Chen, G., 2019. A solar-heat-driven ejector-assisted combined compression cooling system for multistory building – Application potential and effects of floor numbers. Energy Convers. Manag. 195, 86–98. https://doi.org/10.1016/j.enconman.2019.04.090.

Yan, C., Yang, X., Xu, Y., 2018. Mathematical explanation and fault diagnosis of low delta-T syndrome in building chilled water systems. Buildings 8. https://doi.org/10.3390/buildings8070084.

Zhao, H., Yuan, T., Gao, J., Wang, X., Yan, J., 2019. Conventional and advanced exergy analysis of parallel and series compression-ejection hybrid refrigeration system for a household refrigerator with R290. Energy 166, 845–861. https://doi.org/10.1016/j.energy.2018.10.135 https://doi.org/https://doi.org/.